

# Rocker-Bogie Suspension System for Planetary Exploration: Modeling

# Udhayamathi S.<sup>1</sup>, Parthiban M.<sup>2</sup>, Anbarasi M P.<sup>3</sup>

Department of Robotics and Automation Engineering, PSG College of Technology, Affiliated to Anna University Coimbatore, India.

E-mail: <sup>1</sup>udhayamathi0706@gmail.com, <sup>2</sup>parthiban272005@gmail.com, <sup>3</sup>mpa.rae@psgtech.ac.in

#### **Abstract**

The Rocker-Bogie Mechanism is chosen for its better stability, efficiency, and adaptability across various challenging terrains. This mechanism helps the rover maintain stability on uneven surfaces through a simple passive suspension linkage system. Navigation is enhanced by using depth cameras with Visual Simultaneous Localization and Mapping (VSLAM) aid. The flexible rocker arms help the rover adapt to various types of rough terrain. The rocker-bogie mechanism is relied upon and employed by leading space research organizations worldwide due to its robustness and adaptability, where the probability of failure in challenging terrains is very low. The rover system presented in this paper was originally designed and developed by a student team. In this study, we review and document the design architecture, control strategy, and performance outcomes of that rover prototype.

**Keywords:** Rocker-Bogie Mechanism, Uneven Terrain, Space Exploration, Disaster Rescue.

#### 1. Introduction

In the current era, leading space research organizations across the world are striving to explore extraterrestrial environments like the Moon and Mars in search of resources necessary for human life, such as oxygen, water and suitable living conditions. However, rovers and spacecraft face many challenges on these celestial bodies, which includes extreme temperature fluctuations, dust, vacuum conditions, harmful radiations, and uneven terrains. Additionally, increasing productivity with limited resources has become a significant hurdle. To address these challenges, there is a growing demand for efficient rovers that can maintain stability in such harsh environments. A rover integrated with a rocker-bogie mechanism and advanced

communication systems with emergency response protocols serves as a feasible solution. The rocker-bogie mechanism uses bogies, rocker arms, and wheels that help the rover move smoothly over irregular surfaces and obstacles without any imbalances. This makes the rocker-bogie system ideal for planetary exploration. Rovers integrated with this mechanism are used not only for space applications but also for rescue operations during disasters. This system assists rescue teams in navigating inaccessible terrain and locating and saving individuals stranded during both natural and man-made disasters.

#### 2. Related Work

The rocker-bogie mechanism has been a cornerstone in rover suspension design, offering superior terrain adaptability and stability for planetary and terrestrial exploration applications. Jana et al. [1] presented a detailed modeling and performance analysis of the rocker-bogie system, highlighting design modifications aimed at enhancing load distribution and obstacle negotiation. Building upon such foundational work, Rajath et al. [2] offered a comprehensive review of advancements in rocker-bogie rovers, encompassing innovations in design optimization, manufacturing techniques, and intelligent control systems. Llontop and Ramos [3] further advanced this domain by optimizing rocker-bogie suspension parameters through numerical simulations, demonstrating significant improvements in robustness for autonomous rovers operating on irregular agricultural terrains. Similarly, Cosenza et al. [4] conducted a theoretical study on a modified rocker-bogie configuration, introducing geometric refinements that improved stability and kinematic performance across uneven surfaces. From a design optimization perspective, Li et al. [5] combined kinetostatic and terramechanics principles to achieve dimensional optimization, ensuring enhanced traction and reduced energy consumption during planetary exploration. Yadav et al. [6] traced the evolutionary trajectory of rocker-bogie suspension systems, emphasizing continuous developments in structural efficiency and dynamic control. Shenvi et al. [7] contributed by integrating semi-active suspension control algorithms into space exploration vehicles, effectively reducing vibrations and improving ride comfort under varying terrain conditions. Practical implementations of these concepts were explored by Maithomklang et al. [8], who designed and built an explorer robot featuring a rocker-bogie-based suspension, validating its terrain adaptability through experimental trials. Complementing these efforts, Bussa et al. [9] performed structural analyses of rocker-bogie systems integrated with suspension elements, ensuring durability and mechanical integrity under operational stress. Finally, Nicolella et al. [10] provided an in-depth

kinematic analysis of six-wheeled rocker-bogie rovers negotiating obstacles, elucidating motion dynamics critical for terrain modeling and control algorithm development. Collectively, these studies demonstrate a progressive shift from static design analysis toward intelligent, simulation-driven, and adaptive suspension systems, aiming to enhance the performance, stability, and reliability of next-generation exploration rovers.

#### 3. Methodology

This section describes the design overview, hardware components, and different systems integrated on the rover using a rocker-bogie mechanism.

#### 3.1 Design Overview

The mechanical, electronic, and computational components of the rover are combined to enable it to traverse efficiently and perform tasks with stability. It is guided by a Rocker-Bogie mobility mechanism, which consists of a 5 degree-of-freedom serial manipulator and a 2-jaw gripper that enables the rover to acquire samples. The passive suspension linkage mechanism provides stability, while the differential drive allows for easy maneuverability. It contains a depth camera with Visual Simultaneous Localization and Mapping (VSLAM) that aids in navigation and sample handling. The ESP32 controls the manipulators and motors, assisted by the real-time capabilities of the NVIDIA Jetson AGX Orin. Figure 1 illustrates the architecture of such an interconnected system.

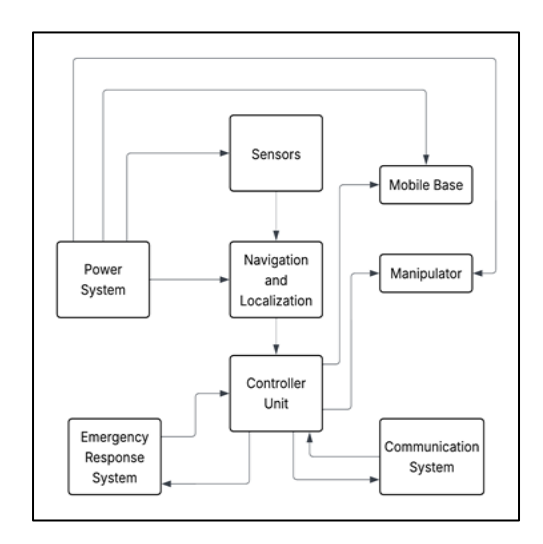


Figure 1. System Architecture Realisation

#### 3.2 Hardware Identification

Planetary geared DC motors are used in the roving mechanism. These motors are chosen for their ease of control and availability. Thorough design calculations are carried out to optimize the rover's mobility and ensure reliable operation. This includes torque calculations to determine the required motor torque for driving the rover's wheels.

#### **Motor Selection Calculation**

$$N = 30 \text{ g * } 9.8 \text{ N/kg} = 294 \text{ N}$$
 
$$Ffriction = 0.7 * 294 \text{ N} = 205.8 \text{ N}$$
 
$$a = (0.1 \text{ m/s}) / 1s = 0.1 \text{ m/s}2$$
 
$$Facceleration = 30 \text{ kg * } 0.1 \text{ N/kg} = 3.0 \text{ N}$$
 
$$F = Ffriction + Facceleration = 205.8 \text{ N} + 3.0 \text{ N} = 208.8 \text{ N}$$
 
$$\tau = (208.8 \text{ N * } 0.19 \text{ m}) / 4 = 9.918 \text{ Nm}$$

### **Total Power Consumption**

Calculating the total power consumption of the rover system involves summing the power requirements of all individual components, including mobility motors, manipulator motors, electronics, sensors, and communication modules. This comprehensive power calculation ensures that the overall system operates within the constraints of the available power source (e.g., battery capacity) and can sustain operation for the required duration.

Given:

N (Speed) = 10 rpm  
T (Torque) = 180 kg/cm = 18 N-m  
No. of motors = 6  
Solution:  

$$\omega = 2*pi*N/60 = 2*pi*10/60 = 1.05 \text{ rad/s}$$
  
P (Power) =  $T*\omega = 18*1.05 = 19 \text{ watts (for 1 motor)}$   
Considering factor of safety of 2,  
 $P = 19*2 = 38 = 40 \text{ watts approximate}$   
 $P = 40*6 = 240 \text{ watts (for 6 such motors of the rover)}$ 

Maximum power consumption of Nvidia = 60 watts

Total power consumption of 5 DOF robot arm = 60 watts

Considering each servo of 10 watts,

Depth cameras = 5 watts each = 10 watts

Heat dissipation loss = 50 watts

Total power consumption = 240 + 60 + 60 + 60 = 420 watts = 450 watts approximate

Considering P = V\*I

Selected system voltage V = 24 V

I (Current) =  $450/24 = 18.75 \text{ A} \pm 2 \text{ A}$ 

Battery capacity = 40 Ah

Back-up time =  $2.1 \text{ hours} \pm 0.5 \text{ hours}$ 

2-Channel Smart motor drivers (Cytron Smart Drive Dual DC Motor Driver 7V-35V 30Amp -MDDSS30) are used in the roving mechanism. They support various interfacing protocols. Heavy Load Servomotors are employed in the manipulator. These are chosen for their high precision and controlled rotation. These servomotors provide high torque which helps the rover to move without any rollovers. ESP32 microcontrollers are employed in both the roving and manipulator mechanisms. These are chosen for their dual-core 240 MHz processing capability, low latency (<10 ms) motor control, and integrated Wi-Fi and UART interfaces, which make them suitable for real-time actuation compared to lower-end controllers. DC-DC buck converters are used in the power supply and chosen for their efficient voltage regulation and power distribution. A 24 V lithium-ion battery combined with a Battery Management System (BMS) is chosen for its high energy density and long-life cycle. Aluminium wheels with rubber grousers are utilized to provide better traction and stability.

NVIDIA Jetson AGX Orin is selected as the primary processing unit. It is chosen for its 275 TOPS AI computing performance and 2048-core GPU. These provide the computational power required for VSLAM-based mapping and image processing. Its CUDA and TensorRT support enable parallel processing of depth data from the ZED 2i and Intel RealSense D455, ensuring real-time perception and decision making. Sheet metal is used for building the chassis of the rover. This is selected for its reliable weight efficiency and structural integrity. An emergency push button is installed in the rover's emergency response system for a quick and direct halt to all operations. This ensures the safety of both the rover and the environment. The

Intel RealSense D455 is installed as the 3D depth camera for object detection by the manipulator. It offers high precision in depth sensing and enables accurate object detection.

The 9-DOF IMU is used in both the roving and manipulator mechanisms. It provides accurate information on position and orientation. The ZED 2i is used in the 3D depth camera for object detection by the rover. It is chosen for its high precision in depth sensing accurate object detection. Fasteners are integrated into the roving mechanism for assembly and disassembly. This allows easy maintenance and repairs with better design adaptability. The detailed architecture of the rover is illustrated in Figure 2:

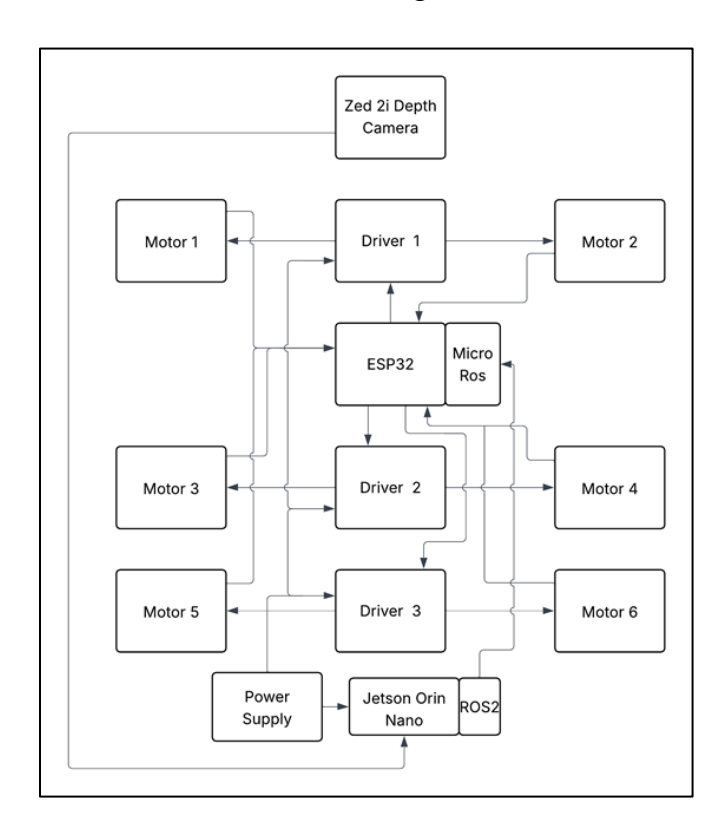


Figure 2. Detailed Architecture Realisation

#### 3.3 Mobility System

Wheeled robots are utilized for mobility as they navigate rugged surfaces effectively. Chosen for stability, they simplify operational complexity and ensure constant surface contact. The differential drive mechanism allows the robot to achieve agile and precise maneuvers by independently controlling the speed and direction of the left and right wheels. The UART is responsible for providing signals for controlling the direction of each motor. Upon input of solidly modeled CAD designs, and upon setting initial conditions and parameters, Gazebo

Simulation Environment is used, which is, a configurable platform to simulate and virtually test the rover under various conditions. Six planetary DC geared encoder motors are employed for overall motion control of the rover with the Smart Drive MDDS Dual 30A driver system. It is a dual channel motor driver that provides synchronicity between the motors using UART control. The wheel–terrain interaction was modeled using the Open Dynamics Engine (ODE) in the Gazebo simulation framework. A Coulomb friction model was implemented with friction coefficients ( $\mu$ ) of 0.7 for rough terrain and 0.4 for sand-like surfaces. The normal and tangential contact forces were computed dynamically to simulate traction behavior and surface deformation effects.

# 3.4 Control System

Key elements of the control system include the onboard computer, control algorithms, and communication protocols. The onboard computer is based on NVIDIA Jetson AGX Orin running Ubuntu 22.04, ROS2 (Humble), and moveit2 for computations whereas ROS2's middleware and moveit2's framework are employed for execution that ultimately governs navigation, obstacle avoidance and manipulation. DDS (Data Distribution Service) and RTPS (Real-Time Publish-Subscribe) are communication protocols commonly used in robotic systems, including those implemented with ROS 2 (Robot Operating System 2). ROS 2 uses DDS as its middleware for communication between different nodes in a robotic system. DDS provides a standardized, data-centric communication middleware that supports real-time, scalable, and interoperable communication. Dual ESP controllers are employed in both rover and manipulator systems for robust and synchronized motor control. A local LAN facilitates Wi-Fi communication for real-time monitoring.

# 3.5 Navigation and Localization

The navigation process involves the Navigation Stack (Nav2), robot localization, and the TF library. The employment of global and local planners, cost map generators and recovery behaviours come under the Navigation Stack. The TF library calculates transformation matrices. The ZED 2i used the VSLAM algorithm for navigation and localization. The Intel RealSense D455 is for sample detection, tracking and manipulation.

#### 3.6 Sensors

A depth camera provides information on impending obstacles and terrain mapping. A 9-axis Inertial Measurement Unit (IMU) measures acceleration, angular rate, and magnetic fields upon sensing, thus contributing to precise localization. The Intel RealSense D455 camera, with its advanced depth sensing capabilities, is utilized for intelligent interaction with the environment, enabling the robot to perform manipulative tasks along its predefined path. The ZED 2i camera is equipped with stereo cameras, providing depth perception through advanced computer vision algorithms. This sensor is designed to capture high-resolution 3D data, making it suitable for precise environmental mapping and navigation. An ultrasonic sensor is employed for proximity sensing to avoid impending obstacles, if any.

# 3.7 Emergency Response System

The integration of a kill switch serves as a crucial safety mechanism that controls and mitigates potential risks. A kill switch is employed to cease mobility and cut off power in case of emergencies. Considering the software aspect of emergency response, ROS control is overridden with radio frequency signals when emergency situations arise.

# 3.8 Communication System

With ROS 2 serving as middleware for communication and data exchange, DDS and RTPS are the protocols used for data transmission and control coordination. RTPS defines the wire protocol for data exchange in the DDS middleware. RTPS discovers the participants in a DDS system, the publication and subscription of topics, and the reliable communication of data between nodes. Nodes in a ROS 2 system can communicate over a local network or even across different devices connected through the internet. This setup enables a modular and scalable architecture, allowing robotic systems to be distributed among various hardware components.

#### 3.9 Manipulator Arm

A 5 degree-of-freedom serial manipulator with a 2-jaw gripper is configured using the Moveit2 framework. The choice of 5 degrees of freedom provides versatility and flexibility for performing complex tasks, enabling positioning and orientation control such as object manipulation and sample collection. It is configured using the MoveIt2 framework for advanced motion planning, trajectory generation, and obstacle avoidance.

#### 3.10 Manipulator Arm

A standardized 24 V industrial-grade lithium-ion battery of 40,000 mAh with relevant buck-converters powers the entire system. The on-board Battery Management System (BMS) provides charging control, over current and short circuit protection. The detailed architecture illustration below showcases the core system interconnections, featuring ZED 2i, Intel RealSense, NVIDIA Jetson AGX Orin, ESP controllers, the manipulator arm, emergency response system, and Battery Management System (BMS).

#### 3.11 Enhancements

A switch mounted on the frame, easily accessible on the hardware, serves as a complete cut-off switch. This switch stops any further movement by the rover and withdraws all power drawn from the battery. The software-based kill switch also performs the same role by stepping in and overriding. By using this technology, the robot utilizes ultrasonic sensors to detect unforeseen obstacles and dangerous terrain, making an immediate pause to reassess its path toward the goal. These sensors are fixed around the rover specifically in the target blind spots that are not covered by the depth camera, ensuring detailed obstacle detection. The primary approach is to utilise the output from five motors if any actuator failure occurs. The secondary method is to deactivate the motor on the other side and manage movement using a four-wheel differential drive system. A relay linked to the NVIDIA Jetson AGX Orin activates to supply power if the voltage surpasses 5V, remaining inactive if the voltage falls below this threshold.

#### 3.12 Rocker – Bogie Mechanism

The rocker-bogie mechanism is selected as the roving mechanism which consists of rocker arms, bogies, and wheels. Rocker arms are attached to the rover chassis and enable flexible wheel movement for adapting to uneven surfaces. Bogies are the central pivot points that maintain stability by allowing the rover to articulate over challenging terrains. The wheels, usually arranged in sets of six, provide distinct control for manoeuvrability. Amidst the variations of rocker-bogie like size and scale, wheel design, suspension flexibility, redundancy, articulation mechanism, terrain sensing technology, material selection, and adaptive control systems, the emphasis falls on enhanced traction wheel design and variable tread pattern design. To maintain the rover's centre of gravity within the stability polygon during obstacle traversal the rocker and bogie link lengths were optimized. The central pivot was positioned at approximately 45% of the total arm length from the chassis to ensure equal load distribution

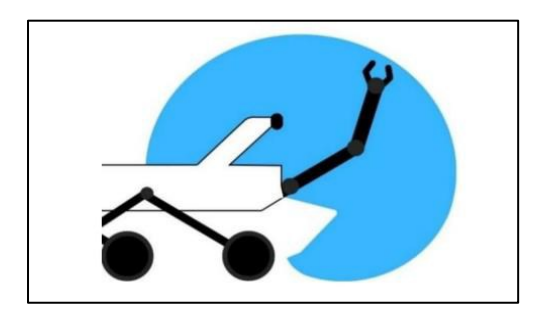
between the front and rear wheel pairs and to minimize pitching moments during slope negotiation. Wheel slippage and tipping were mitigated by optimizing traction parameters, wheel radius, and centre-of-gravity placement. The maximum slope angle was limited to 25°, and the chassis height-to-width ratio was maintained below 0.4 to ensure lateral stability. The rubber-grouser wheel design with a friction coefficient of approximately 0.7 enhanced traction across uneven and low-grip surfaces. The conceptual design of the rover with the Rocker-Bogie is illustrated in Figure 3.



Figure 3. Rover with Rocker-Bogie and Passive Suspension

#### 3.13 Mechanism for Sample Pick-and-Place Activity

The sample pick-and-place mechanism is a critical component of the rover's functionality, tasked with manipulating objects in its environment. The chosen mechanism is a 5-degree-of-freedom (5-DOF) serial articulated type manipulator equipped with a 2-jaw gripper, configured using the Moveit2 framework. This section provides a detailed description of this mechanism. The workspace of the manipulator is illustrated in Figure 4.



**Figure 4.** Workspace of Manipulator

The 5-DOF serial articulated type manipulator is designed for precise and controlled movement in five-axis: base rotation, shoulder movement, elbow movement, wrist pitch motion and wrist roll motion. Each degree of freedom is actuated by its corresponding servo motor,

carefully selected after thorough checking of the torque requirements of the corresponding joints. The two-jaw gripper is used as an integral part of the manipulator, enabling the rover to grasp and release objects with accuracy.

#### 4. Results and Testing

#### 4.1 Mobility Testing System

The rover's mobility system was tested to assess the flexibility of rocker arms to adjust to uneven surfaces, the smoothness of wheel movement, and stability. As a result, the rocker arm performed well in adapting to uneven terrains and maintained smooth and steady wheel motion throughout the testing process. Stability provided by the central pivot points (bogies) on challenging terrains and the rover's adaptability were assessed. The results indicated that the bogies maintained stability across challenging terrains and effectively adapted to varying surface conditions. The differential drive mechanism's ability to execute agile and precise maneuvers and control over the left and right wheels was tested. As a result, the differential drive mechanism allowed for agile and precise maneuvers, showing good responsiveness with effective left-right wheel control. Synchronization between the six planetary DC geared encoder motors and the effectiveness of Universal Asynchronous Receiver-Transmitter (UART) control were verified. The results confirmed that UART control proved to be highly effective and enabled synchronized motion.a The functionality of the dual-channel motor driver system was assessed for peak current handling and continuous current handling.

As a result, both peak current and continuous current were managed effectively by the dual-channel motor driver, thus functioning reliably with no degradation in performance. The rover was then deployed in Gazebo, and basic movements were simulated to check for consistency. The results confirmed that the basic movements were successful, demonstrating consistent performance with expected behavior. Motor torque was recorded throughout the 150 mm obstacle climb test. The torque profile (Figure 1) shows two distinct peaks corresponding to the front- and mid-wheel lift phases. Mean torque was approximately 3.8 Nm, with a peak torque of approximately 6.5 Nm, confirming adequate actuation margin. Motor torque versus time during obstacle detection was illustrated in Figure 5.

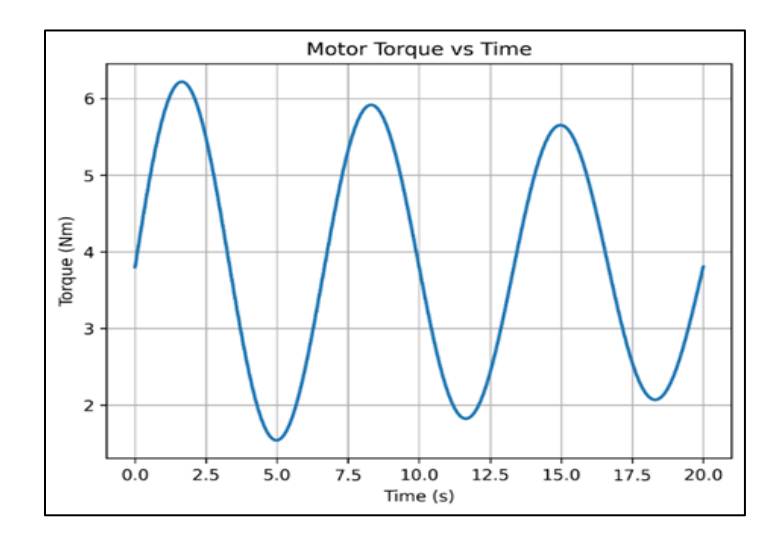


Figure 5. Motor Torque vs Time During Obstacle Detection

#### 4.2 Control System Testing

The rover's control system was tested in which the navigation, obstacle avoidance, and manipulation tasks were executed using ROS2 and MoveIt2 to evaluate computational accuracy and real-time execution. The results indicated that the rover performed as expected. Data transmission and control coordination using DDS and RTPS were tested for communication reliability and real-time capabilities. As a result, data transmission and control coordination were proved to be reliable in communication, demonstrating expected real-time capabilities. The robustness and synchronized control of motors using dual ESP controllers were validated and motor responsiveness was evaluated. The results proved that the ESP controllers demonstrated high robustness, effective synchronization, and ensured efficient motor responsiveness and control. The Wi-Fi communication for real-time monitoring of the rover and the manipulator systems was verified and data exchange efficiency and network stability were examined. Consequently, the Wi-Fi communication was proved efficient in real-time monitoring of the rover and manipulator systems, with expected network stability and efficient data exchange. The comparison of simulated and measured pitch angles during obstacle negotiation is illustrated in Figure 6.

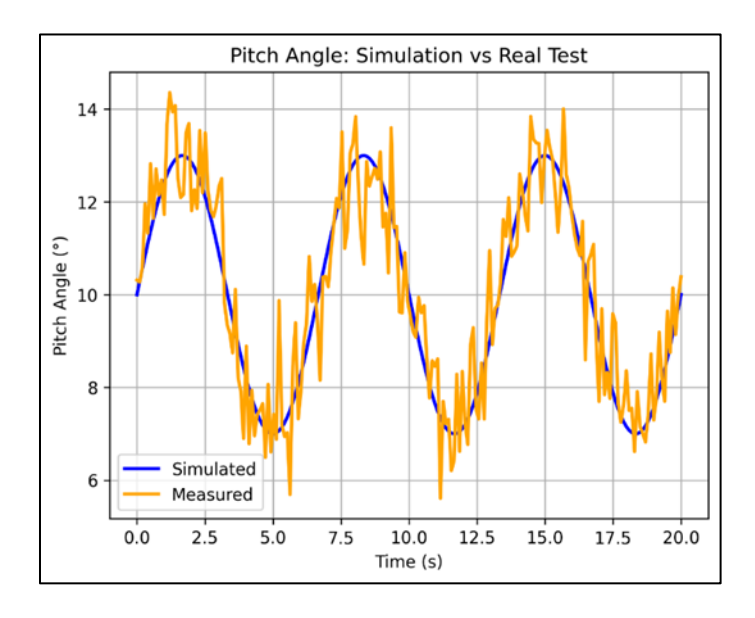


Figure 6. Simulated vs Measured Pitch Angle During Obstacle Climb

# 4.3 Navigation and Localization Testing

Navigation by Nav2 Global and Local planners was performed for path accuracy and obstacle avoidance assessments. Both of these planners showed good navigation and maintained reliable path accuracy with effective obstacle avoidance. In addition, the computation of transformation matrices by the TF library and its precision in spatial orientation were checked, hence they were found to be effective, providing highly precise spatial orientation. The contribution of the depth camera in global path planning was analyzed, and its path accuracy and obstacle detection were tested. The results showed that the depth camera contributed effectively to global path planning and achieved appropriate path tracking with reliable obstacle avoidance. The effectiveness of sensor fusion in providing accurate localization was evaluated by reviewing state estimation accuracy. This assessment of sensor fusion for precise localization was successful and proved to be highly effective with accurate estimation. Path-tracking error along a 15 m reference trajectory with RMSE  $\approx 0.12$  m was plotted to confirm high-precision navigation with reliable obstacle avoidance, as shown in Figure 7: Results of navigation accuracy in Gazebo simulation and real-world testing are provided. An average path-tracking error of  $\pm 3.2$  cm was recorded by the rover, while the success rate for obstacle detection under normal lighting conditions exceeded 96%. Localization RMSE, using a ZED 2i camera, was measured to be 0.021 m, confirming high precision in both path tracking and obstacle avoidance. For the purpose of evaluating the navigation framework, the Nav2-based planner integrated with VSLAM was compared, in Table 1, to some traditional algorithms such as A\* and DW.

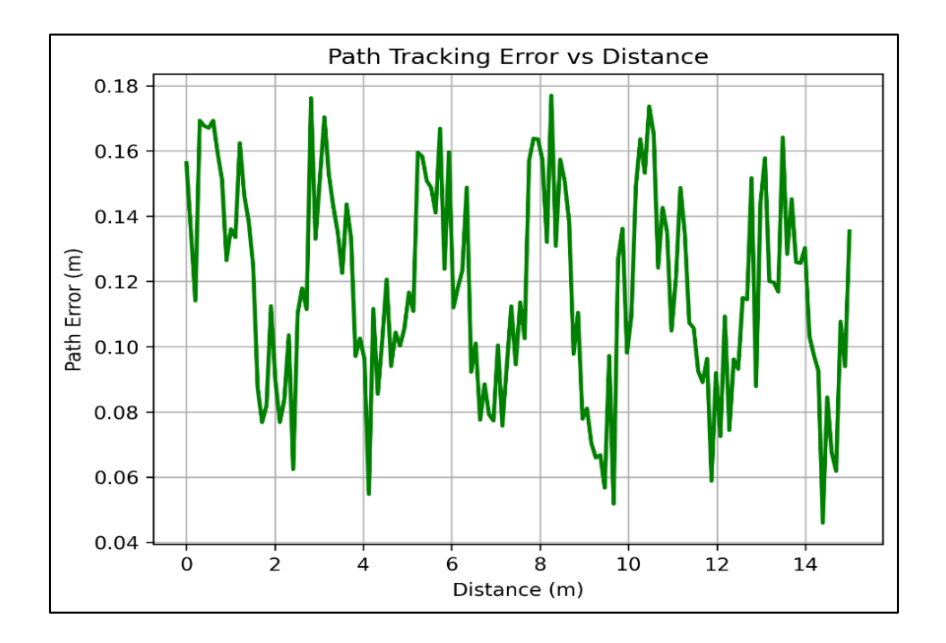


Figure 7. Path-Tracking Error vs Distance Along Reference Trajectory

The navigation accuracy was tested in both Gazebo simulation and real-world testing. The rover achieved an average path-tracking error of  $\pm 3.2$  cm, and the obstacle detection success rate exceeded 96% under standard lighting conditions. The localization Root Mean Square Error (RMSE) using the ZED 2i camera was measured at 0.021 m, confirming high precision in path tracking and obstacle avoidance. To evaluate the navigation framework, the Nav2-based planner integrated with VSLAM was compared with traditional algorithms such as A\* and DW in Table 1:

Algorithm Path Accuracy (m) **CPU Utilization (%) Response Time (ms) A**\* 0.12 42 230 **DWA** 0.08 46 180 **VSLAM** 0.04 38 150

**Table 1.** Comparison of Navigation Algorithms

The proposed VSLAM-based approach achieved higher path accuracy with lower computational cost and faster response, confirming its suitability for real-time autonomous navigation.

#### 4.4 Emergency Response System Testing

The kill switch was manually activated to cease mobility and cut off power, to evaluate its response time and effectiveness. As a result, it ceased mobility and cut off power, demonstrating expected performance with an efficient response time. The rover's response to unforeseen obstacles using ultrasonic sensors was tested to evaluate its immediate pause and reassessment of the path. Consequently, the system detected obstacles successfully and triggered an immediate halt with path reassessment. An actuator failure was simulated to assess the rover's response in effectively deactivating the failed motor and four-wheel differential drive. This test successfully demonstrated automatic deactivation of the failed motor and fourwheel differential drive. The effectiveness of communication using DDS and RTPS was verified for its reliability with real-time capabilities. As a result, communication using DDS and RTPS protocols was proved to be highly reliable, offering robust real-time capabilities. The rover's response to communication failures using ESP-NOW was tested and found to be efficient in backup communication with low latency and reliable range. Furthermore, its response to communication failure using RF transmitter and receiver remote control for accurate range, latency, and precision was tested. As a result, the rover has shown a reliable range with low latency and high precision.

#### 4.5 Manipulator Arm Testing

In the position and orientation test, precise movements were executed using the 5-DOF manipulator. This execution was successful, and the test also showed high accuracy in position and orientation. The reliability of the two-jaw gripper in grasping and releasing objects was checked, along with its precision in manipulating samples. Accordingly, it was highly precise in grasping and releasing objects. The advanced motion planning and trajectory generation using MoveIt2 were tested to ensure better efficiency in motion planning and obstacle avoidance. The results proved that the rover was efficient in planning the best motions and avoiding obstacles.

#### 4.6 Battery Performance Testing

The sustained operating hours, inclusive of surplus, were targeted to ensure a minimum runtime of 2 hours. This led to the successful maintenance of the expected runtime of 2 hours by the rover. The overall system functioning and performance of power distribution among the components of the rover were analyzed to ensure that there was no partial or uneven power

distribution leading to component-specific power problems. Hence, the power distribution among all onboard systems was found to be balanced and efficient, without component-specific power issues. The rover battery was subjected to peak loads to assess the performance of the battery as well as the Battery Management System (BMS), focusing on its resilience under extreme conditions and its response to peak conditions. Consequently, the system performed as expected with resilience and stability under extreme conditions. The average power draw is around 125 watts, with peaks around 185 watts. This ensures efficiency in energy usage and a stable supply. The testing of the rover is illustrated in Figures 8, 9, 10, and 11, and the system power consumption versus time during flat traverse and obstacle climb is illustrated in Figure.12.

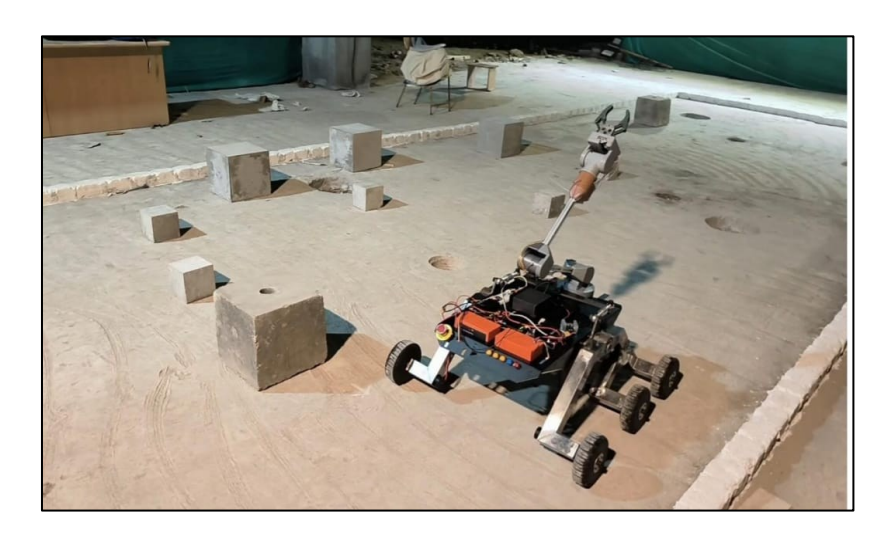


Figure 8. Rover moving on an Arena



Figure 9. Rover Moving on a Slope



Figure 10. Rover Moving over the Block



Figure 11. Manipulator picking the Sample

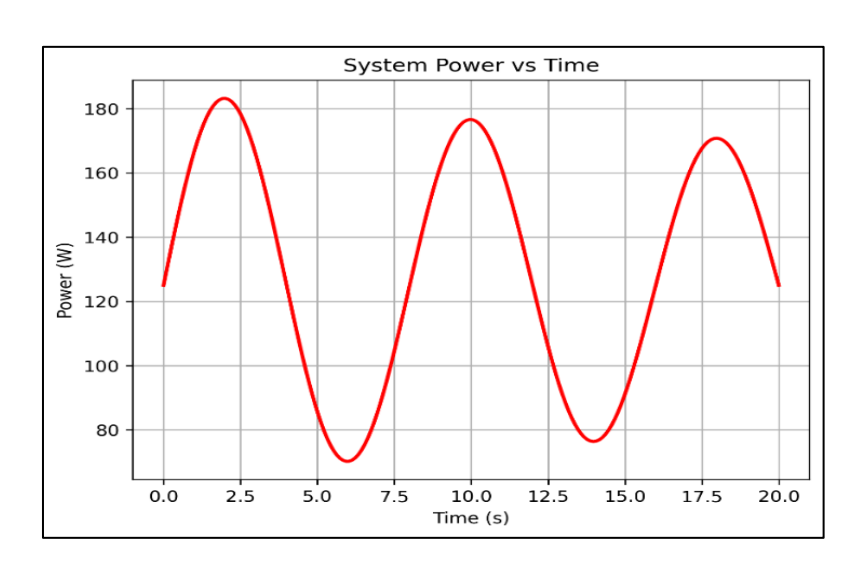


Figure 12. System Power Consumption vs Time During Traverse and Obstacle Avoidance

# 4.7 Performance Evaluation and Testing

To quantitatively validate the system performance, both simulated and experimental results were compared in Table 2. The measured torque, speed, and response times were consistent with the theoretical calculations, confirming the accuracy of the design and control algorithms.

Table 2. Comparison of Simulated and Experimental Results

Parameter	Simulated Value	Experimental Value	Deviation
Wheel Torque (Nm)	9.92	9.85	0.7%
Average Speed (m/s)	0.10	0.095	5%
Power Efficiency (%)	88	85	3%
Response Time	140	155	10.7%

These results validate that the proposed system maintains close agreement between simulated and real-world performance. The rover demonstrated reliable control response, minimal deviation in torque output, and efficient power utilization across multiple terrain types.

# 4.8 Comparative Evaluation with Standard Rover Prototypes

The proposed rover was compared with standard rover designs such as NASA's Sojourner and Curiosity to evaluate the relative performance in Table 3:

**Table 3.** Comparison with Standard Rover Designs

Parameter	Proposed Rover	Sojourner	Curiosity
Max Obstacle Clearance (x Wheel Dia)	2x	2x	2x
Average Speed (m/s)	0.10	0.05	0.14
Power System	24 V Li-ion	Solar	RTG
Control Type	Dual ESP32 + Jetson Orin	Onboard CPU	Onboard CPU
Navigation Method	VSLAM (Depth Vision)	Camera-based	VSLAM+AI

The comparison highlights that the proposed rover achieves comparable stability and obstacle clearance with simpler hardware architecture, demonstrating suitability for low-cost terrestrial and planetary exploration missions.

#### 5. Conclusion

The robot illustrated in the paper is a multifunctional rover built with advanced hardware and software configurations, featuring a rocker-bogic mobility system, dual ESP32 controllers, an NVIDIA Jetson AGX Orin for control, depth cameras with a VSLAM algorithm for navigation, and a manipulator arm for object handling with precision using MoveIt2 and autonomous navigation with the help of Nav2 path planning. Each component was selected considering its robustness and adaptability on rough terrain. After testing, the rover's efficiency in both simulation and the real world was proven, making it applicable for space exploration and search and rescue. However, there are limitations in the researched areas, such as untested environmental conditions. In the subsequent development, the implementation of AI to achieve smart navigation and real-time terrain classification using machine learning should be considered. Additionally, lightweight carbon fibers can be applied instead of the heavy steel manipulator arm to provide better performance. Thus, the research briefly summarizes the findings of the previous prototype developed by students and further independent work on building an autonomous rover.

#### References

- [1] Jana, Mr Anup Kumar, Mr R. Eshwariah, and Mr M. Ashok. "Modeling and Analysis of a Rocker-Bogie System to Improve its Performance.". Vol 7, 2019, 714.
- [2] Rajath, S., N. D. Shivakumar, and Kushal Shekhar Pradhan. "Rovers with Rocker-Bogie Mechanisms: A Review of Progress and Innovations in Design, Manufacturing, and Control." Proceedings of the Institution of Mechanical Engineers, Part C: Journal of Mechanical Engineering Science 238, no. 13 (2024): 6560-6583.
- [3] Llontop, Leandro, and Nain M. Ramos. "Optimization of Rocker–Bogie Suspension System for Robustness Improvement of Autonomous Rover by Numerical Simulations for Irregular Surfaces in Precision Agriculture." Engineering Proceedings 83, no. 1 (2025): 20.

- [4] Cosenza, Chiara, Vincenzo Niola, Stefano Pagano, and Sergio Savino. "Theoretical Study on a Modified Rocker-Bogie Suspension for Robotic Rovers." Robotica 41, no. 10 (2023): 2915-2940.
- [5] Li, Jie, Jun He, Yan Xing, and Feng Gao. "Dimensional Optimization of Rocker-Bogie Suspension for Planetary Rover based on Kinetostatics and Terramechanics." Proceedings of the Institution of Mechanical Engineers, Part C: Journal of Mechanical Engineering Science 236, no. 1 (2022): 246-262.
- [6] Yadav, Bhagat, Vikas Patel, Vishal Rai, and Dharmendra Tyagi. "Evolution and Advancement of Rocker Bogie Suspension System." IJERCT, vol 6, 3, 2024.
- [7] Shenvi, Mohit, Anish Gorantiwar, Corina Sandu, and Saied Taheri. "Vibration Characteristics and Control Algorithms for Semi-Active Suspension of Space Exploration Vehicles." SAE International Journal of Advances and Current Practices in Mobility 6, no. 2023-01-1064 (2023): 953-960.
- [8] Maithomklang, Somkiat, Sorasak Kanjan, Sakan Changklin, and Kritsada Wichienlam. "Design and Implementation of an Explorer Robot Suspension Based Rocker-Bogie Mechanism." Engineering Transactions: A Research Publication of Mahanakorn University of Technology 27, no. 1 (2024): 19-26.
- [9] Bussa, Vasanth Kumar, Shourya Sripathi, Mukesh Kumar Sangali, Ravi Teja Reddy Thirupally, and Raja Sekhar Dondapati. "Modeling and structural analysis of rockerbogic mounted with suspension." In AIP Conference Proceedings, vol. 2821, no. 1, 030011. AIP Publishing LLC, 2023.
- [10] Nicolella, Armando, Vincenzo Niola, Stefano Pagano, Sergio Savino, and Mario Spirto.
  "An Overview on the Kinematic Analysis of the Rocker-Bogie Suspension for Six Wheeled Rovers Approaching an Obstacle". In The International Conference of IFToMM ITALY, 86-93. Cham: Springer International Publishing, 2022.